Electron-energy-loss cross-section and surface lattice-dynamics studies of NiAl(110)

Y. Chen, M. L. Xu,* and S. Y. Tong
Department of Physics and Laboratory for Surface Studies, University of Wisconsin–Milwaukee, Milwaukee, Wisconsin 53201

M. Wuttig, W. Hoffmann, R. Franchy, and H. Ibach
Institut für Grenzflächenforschung und Vakuumphysik, Kernforschungsanlage Jülich, Postfach 1913, D-5170 Jülich 1, Federal Republic of Germany

(Received 1 May 1990)

We use a multiple-scattering theory [Phys. Rev. Lett. **44**, 407 (1980)] to analyze the electron-energy-loss cross section for the (110) surface of the ordered alloy NiAl. The study indicates that the interatomic forces in the near-surface region are significantly different from the bulk values. We determine a surface lattice-dynamical model which produces good fit to the measured phonon-dispersion curves as well as the electron-energy-loss cross sections. The analysis shows that along the $\bar{\Gamma}\,\bar{Y}$ (i.e., [100]) direction, the polarizations of the two lowest-frequency surface modes are interchanged as they approach the Brillouin-zone boundary. The calculated inelastic-electron-scattering cross sections show significant sensitivity to the surface structure.

I. INTRODUCTION

The surface-phonon vibrations for the (110) face of the ordered alloy NiAl have been studied with use of high-resolution electron-energy-loss spectroscopy (EELS) both in the [100] ($\bar{\Gamma}\,\bar{Y}$) and [110] ($\bar{\Gamma}\,\bar{X}$) directions. This is the first time that surface-phonon dispersions for a compound with CsCl crystal structure have been measured. The experimental details and a discussion of the surface lattice-dynamical model used to fit the phonon dispersion curves are presented in the preceding paper[1] (hereafter referred to as I).

In the high-resolution EELS technique, measured surface-phonon dispersion curves are commonly generated by determining electron-energy-loss peak positions as a function of phonon wave vector. The procedure is valid if the frequency of the surface mode is well separated from bulk or resonance bands. For surface modes which are close to bulk bands, the measured energy-loss peaks are often shifted from their actual frequencies due to the neighboring bulk and resonance modes. In a complicated system where a number of surface and resonance modes appear closely together, the determination of the phonon dispersion curves directly from the measured electron-energy-loss spectra becomes difficult and unprecise. A more precise way is to compare the measured electron-energy-loss spectra with a calculated spectra. Thus, the contribution of each mode to the energy-loss cross section can be individually determined. The frequency and dispersion curve of each mode, no matter how close it is to other modes, can be individually determined and plotted. The dependence of the mode's energy-loss cross section to the incident-electron energy, scattering geometry, and phonon wave vector can be determined and mapped in detail. In this paper we shall report the results of such a study for the ordered alloy NiAl(110).

Another reason for carrying out detailed electron-energy-loss cross-section analysis is that lattice-dynamical models based on force constants are hardly unique. Thus, more than one set of force constants may fit a set of measured dispersion curves satisfactorily. With cross-section analysis, we further require that the optimal lattice-dynamical model to produce surface, bulk, and resonance modes whose calculated electron-energy-loss cross sections must fit the data at different wave vectors, scattering geometries, and incident-electron energies. We have earlier shown that the cross sections are sensitive functions of the scattering conditions.[2–4] Thus, we are imposing much more severe constraints on the chosen set of force constants. We shall show in this paper that such constraints to fit the EELS cross section reveal a striking feature in the Rayleigh mode of NiAl(110).

We shall also show that the calculated EELS cross sections are sensitive functions of surface structure. Thus, in order for the calculated EELS cross sections to fit the data, we must have (i) a surface lattice-dynamical model that produces frequencies in good agreement with the data, (ii) the vibrational displacements and polarizations of the phonons must be correct (to the extent that they produce the correct EELS cross sections at different incident energies, phonon wave vectors, and scattering geometries), and (iii) the surface atomic geometry must be correct. We shall show how these conditions are achieved for the NiAl(110) case. Conversely, we can start with conditions (i) and (ii) and use the comparison of the EELS cross sections with data to determine surface geometry. Such a study was done for the Ni(001)-$c(2\times2)$S system.[5]

In Sec. II we shall describe the choice of the optimal force-constant model used for the (110) surface of NiAl. Section III contains the analysis of the electron-energy-loss cross sections and the comparisons with experiment. In Sec. IV the sensitivity of the EELS cross sections to

surface geometry is presented. Section V contains a summary.

II. SURFACE LATTICE-DYNAMICAL MODEL

NiAl has the CsCl crystal structure. The unit cell of the (110) surface consists of one nickel atom and one aluminum atom per layer. As discussed in paper I,[1] along the [100] ($\bar{\Gamma}\,\bar{Y}$) and [110] ($\bar{\Gamma}\,\bar{X}$) directions, all phonon modes can be classified as being either odd or even with respect to the symmetry plane. We characterize each surface mode by its largest atomic displacement amplitude at the high-symmetry points, such as $\bar{\Gamma}$, $\bar{X}$, and $\bar{Y}$. If the phonon modes are dominated by the displacement of the first-layer Ni (i.e., heavier) atoms, we call these modes the perpendicular shear mode ($SH_{\perp}$) (i.e., the first-layer nickel atoms vibrate perpendicularly to the surface), the shear horizontal mode ($SHO_{\parallel}$, i.e., the odd mode in which the first-layer nickel atoms vibrate parallel to the surface but perpendicular to the wave vector), and the longitudinal mode ($SHE_{\parallel}$, i.e., first-layer nickel atoms vibrate along the wave vector parallel to the surface). If the lighter atoms (i.e., Al), dominate the oscillations, the corresponding shear vertical, shear horizontal, and longitudinal modes are denoted $SL_{\perp}$, $SLO_{\parallel}$, and $SLE_{\parallel}$, respectively. Under in-plane-scattering conditions, the odd modes $SHO_{\parallel}$ and $SLO_{\parallel}$ along the [100] and [110] directions have a zero inelastic-electron-scattering cross section due to selection rules.[2,6]

Mostoller *et al.*[7] have studied the bulk-phonon dispersions for the NiAl crystal experimentally and theoretically. They used three-nearest-neighbor and four-nearest-neighbor Born–von Kármán models to interpret the data. With these models they reproduced the observed bulk-phonon dispersion curves quite well. They also used the three-nearest-neighbor force model to study the gap mode $SL_{\perp}$ at the $\bar{\Gamma}$ point for the NiAl(110), NiAl(111), and NiAl(001) surfaces. We list in Table I the force constants of their third-nearest-neighbor (3NN) model.[7] In their model the third-nearest-neighbor forces have a non-central character (i.e., $\phi_{xx} \neq \phi_{xy} + \phi_{zz}$).

In the force-constant models used for NiAl, the first derivatives of the pair potential (ϕ') are nonzero. This does not create additional constraints in the bulk, because all forces acting on an atom at equilibrium must cancel out, due to the symmetry of the crystal. At the surface, arbitrary choices of ϕ' could result in nonzero net forces on surface atoms. The equilibrium conditions require that the net forces on all atoms due to ϕ' be balanced. It is more convenient to balance forces in a central-force model, and this is what we shall use in this paper.

We first construct a 3NN central-force model based on the bulk force constants of Mostoller *et al.*[7] To do this, we retain the identical first- and second-neighbor $\phi_{\alpha\beta}$'s as those of Mostoller *et al.* We further retain the same ϕ_{xx} and ϕ_{xy} for third-neighbor Ni-Ni forces. The requirement that $\phi_{xx} = \phi_{xy} + \phi_{zz}$ in the central-force model yields ϕ_{zz} for the third-neighbor Ni-Ni interaction. For third-neighbor Al-Al coupling we retain Mostoller's ϕ_{xy}. The value of ϕ_{zz} is obtained from balancing surface forces (see next paragraph). The value of ϕ_{xx} is then obtained from the condition $\phi_{xx} = \phi_{xy} + \phi_{zz}$. A comparison of the force constants between the model of Mostoller *et al.*[7] and our 3NN central-force model is presented in Table I. These two force-constant models produce very similar phonon frequencies. For example, the frequency of the $SL_{\perp}$ mode at $\bar{\Gamma}$ using a bulk-terminated structure is 6.98 THz, calculated by use of the 3NN central-force model. This differs from Mostoller's value of 7.02 THz (Ref. 7) by only 0.04 THz.

TABLE I. Interatomic force constants (units of dyn/cm) in the bulk for a 3NN non-central-force model and a 3NN central-force model. These force constants are expressed in both $\phi_{\alpha\beta}$ and (ϕ'',ϕ') forms. Note that the third-nearest-neighbor forces $\phi_{\alpha\beta}$ in the non-central-force model cannot be converted into (ϕ'',ϕ') form. Here the notation ϕ' should be understood as the first derivative of the pair potential divided by a ($a = 2.887$ Å). The same notation is used in the text.

		Bulk force constants for NiAl (dyn/cm)						
		3NN non-central-force model (Mostoller *et al.*[7])			3NN central-force model (this study)			
Pair	r (Å)	$\phi_{\alpha\beta}$			$\phi_{\alpha\beta}$			
Ni-Al	2.500	(111,xx)	11 240	ϕ''	31 420	(111,xx)	11 240	ϕ''	31 420
		(111,xy)	10 090	ϕ'	1150	(111,xy)	10 090	ϕ'	1150
Ni-Ni	2.887	(200,xx)	2180	ϕ''	2180	(200,xx)	2180	ϕ''	2180
		(200,zz)	−440	ϕ'	−440	(200,zz)	−440	ϕ'	−440
Al-Al		(200,xx)	18 380	ϕ''	18 380	(200,xx)	18 380	ϕ''	18 380
		(200,zz)	760	ϕ'	760	(200,zz)	760	ϕ'	760
Ni-Ni	4.083	(220,xx)	2070	ϕ''	NA[a]	(220,xx)	2070	ϕ''	4760
		(220,zz)	−1370	ϕ'	NA	(220,zz)	−620	ϕ'	−620
		(220,xy)	2690			(220,xy)	2690		
Al-Al		(220,xx)	820	ϕ''	NA	(220,xx)	1276	ϕ''	4036
		(220,zz)	710	ϕ'	NA	(220,zz)	−1484	ϕ'	−1484
		(220,xy)	2760			(220,xy)	2760		

[a]NA denotes not available.

From our 3NN central-force model of Table I, we proceed to balance the forces on surface atoms for a slab having the relaxed, rumpled surface geometry as determined by low-energy electron diffraction (LEED).[8] To satisfy the equilibrium conditions on the surface, we obtain four equations relating five parameters: $\phi'_{\text{Al-Ni}}$(first and second layers), $\phi'_{\text{Al-Al}}$(first and second layers), $\phi'_{\text{Ni-Ni}}$(first and second layers), $\phi'_{\text{Al-Al}}$(first and third layers), and $\phi'_{\text{Ni-Ni}}$(first and third layers). The equilibrium condition within the 3NN central-force-constant model requires that $\phi'_{\text{Ni-Ni}}$(first and third layers) equals the bulk value, i.e., -620 dyn/cm, listed in Table I. We are then left with four parameters which can be uniquely determined by the four equations. The values of ϕ'' and ϕ' in this surface-force-balanced model are listed in Table I of the preceding paper.[1] We denote this model MB. As mentioned in the preceding paragraph, the value of $\phi'_{\text{Al-Al}}$ in the bulk (i.e., -1484 dyn/cm in Table I) has been set to be the same as $\phi'_{\text{Al-Al}}$(first and third layers) to satisfy the equilibrium condition.

We now show phonon frequencies and dispersions calculated from these force-constant models. We use a slab of 15 layers with the relaxed structure as determined by LEED,[8] i.e., the first-layer Al is relaxed outwards by 4.6% and the first-layer Ni inwards by 6%, for the phonon-frequency calculations. As a comparison, the phonon frequencies at points $\bar{\Gamma}$, $\bar{X}$, and $\bar{Y}$ using the 3NN central-force model (Table I) and the 3NN surface-force-balanced model (model MB in Table I, preceding paper) are listed in Table II. We note that simply balancing surface forces produces rather insignificant differences in the phonon frequencies (only ~ 0.1 THz) at the high-symmetry points. The calculated dispersion curves along $\bar{\Gamma}\,\bar{X}$ and $\bar{\Gamma}\,\bar{Y}$ using the MB model are shown in Figs. 7 and 8 of paper I.[1] The large discrepancies between the calculated dispersions and the data have been pointed out in the preceding paper. We shall show in the next section that the electron-energy-loss cross sections calculated from the MB model also are in marked disagreement with the data. It is clear that the bulk-derived force-constant model needs significant adjustments besides balancing the surface forces.

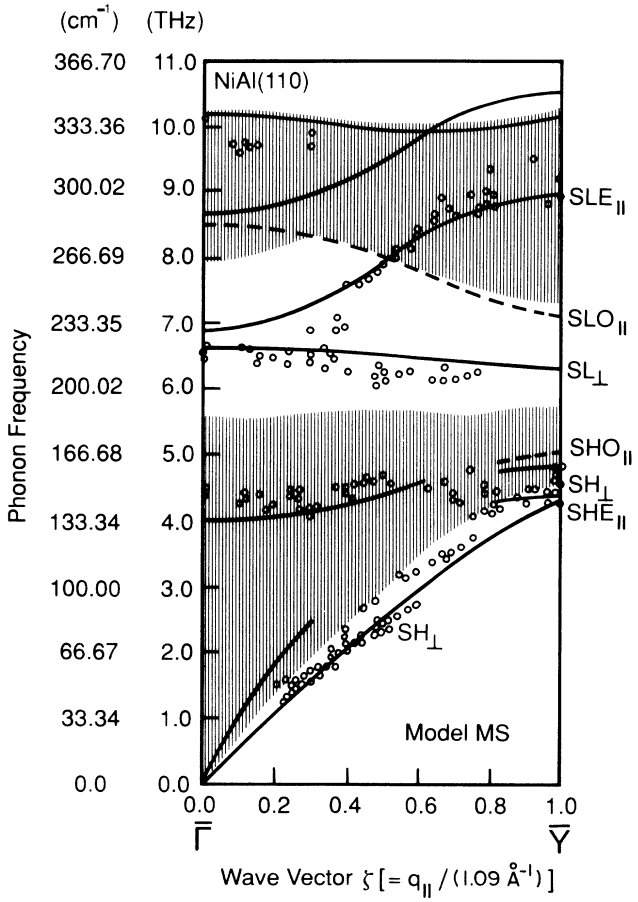

FIG. 1. Calculated phonon dispersion curves for the [100] ($\bar{\Gamma}\,\bar{Y}$) direction using the 3NN central-force surface lattice-dynamical model (the MS model). The surface-layer relaxation and rumpling based on the LEED analysis is assumed for the surface structure. The solid lines are the dispersion of the even surface modes and resonances, and the dashed lines those of the odd surface modes. The experimental data taken at room temperature are indicated as dots.

TABLE II. Phonon frequencies of surface modes at high-symmetry points calculated by various lattice-dynamical models, together with the values measured by use of high-resolution electron-energy-loss spectroscopy. The unit for these frequencies is THz (1 THz = 33.336 cm^{-1} = 4.136 meV).

Surface-phonon model		Surface-phonon frequency (THz)			
		3NN central-bulk-force model	MB model (surface-force balanced)	MS model (surface-force constants)	Expt.
$\bar{X}$	$SH_{\perp}$	2.4	2.4	2.4	2.3
	$SHE_{\parallel}$	5.3	5.2	5.2	5.2
	$SL_{\perp}$	6.6	6.6	6.3	6.3
$\bar{Y}$	$SH_{\perp}$	3.5	3.5	4.4	4.4
	$SL_{\perp}$	6.6	6.6	6.3	
	$SLE_{\parallel}$	9.1	9.1	9.0	9.0
$\bar{\Gamma}$	$SH_{\perp}$	3.6	3.6	4.0	4.3
	$SL_{\perp}$	7.1	7.1	6.6	6.6

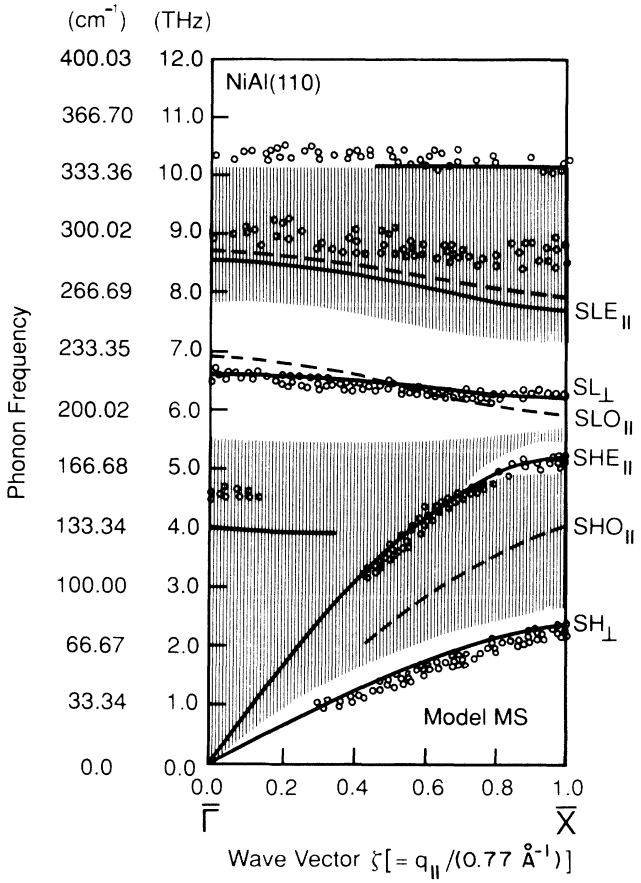

FIG. 2. Same as Fig. 1, but for the [110] ($\bar{\Gamma}\,\bar{X}$) direction.

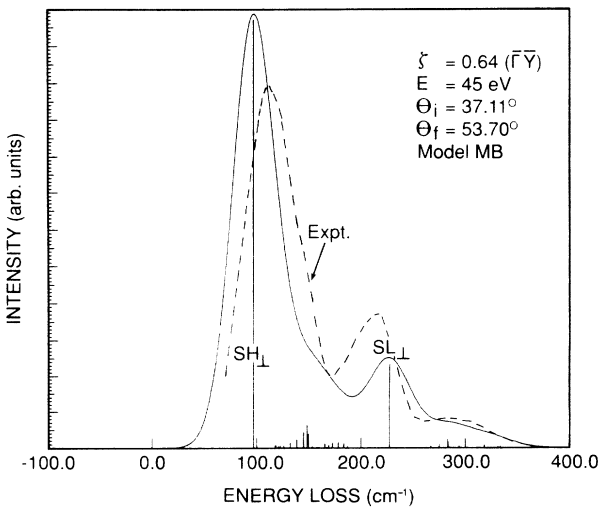

FIG. 3. Calculated (solid line) and measured (dashed line) electron-energy-loss cross-section spectra for incident-electron energy $E=45$ eV and $\zeta=0.64$ along the $\bar{\Gamma}\,\bar{Y}$ direction. Each vertical line represents an individual mode scattering intensity. The atomic-displacement amplitudes and phonon frequencies based on the bulk-force-constant lattice-dynamical model MB are used for the EELS cross-section calculations. The surface-layer relaxation based on LEED analysis is included in the surface structure. The elastic peak at 0 THz is not included in the figure. The calculated (solid) curve is obtained by adding individual mode intensities that are Gaussian broadened; see text.

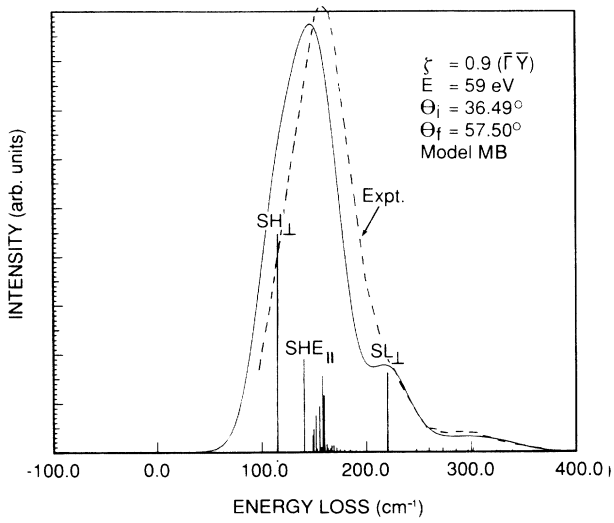

FIG. 4. Same as Fig. 3, but for $E=59$ eV and $\zeta=0.9$ along line $\bar{\Gamma}\,\bar{Y}$.

As discussed in paper I, a surface lattice-dynamical model that produces good fits to the measured phonon dispersion curves *as well as* the electron-energy-loss cross sections (see next section) involves a 20% softening of ϕ''(first-layer Al–second-layer Ni), a 50% increase of ϕ''(first-layer Ni–second-layer Al), a 40% increase of ϕ''(first-layer Ni–second-layer Ni), and a 40% increase of ϕ''(first-layer Ni–third-layer Ni). The signs of these changes are consistent with the relaxed, rumpled surface geometry determined by LEED (Ref. 8) and medium-energy ion scattering (MEIS).[9] In addition to the above changes, we found it is necessary to adjust the intralayer Ni-Ni tangential force constants ϕ' between 2NN to 2000 dyn/cm and 3NN to -2000 dyn/cm. These changes are introduced for the surface-layer Ni only. The adjustment of the intralayer $\phi'_{\text{Ni-Ni}}$(2NN) is responsible for the switching in the polarization of the lowest two surface

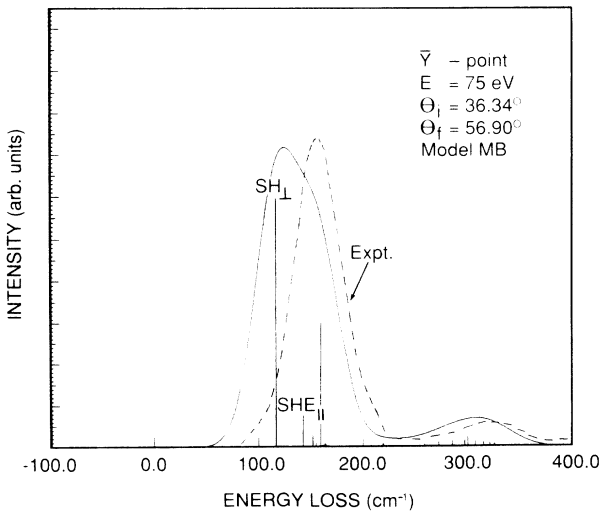

FIG. 5. Same as Fig. 3, but for $E=75$ eV and $\zeta=1.0$ (the $\bar{Y}$ point).

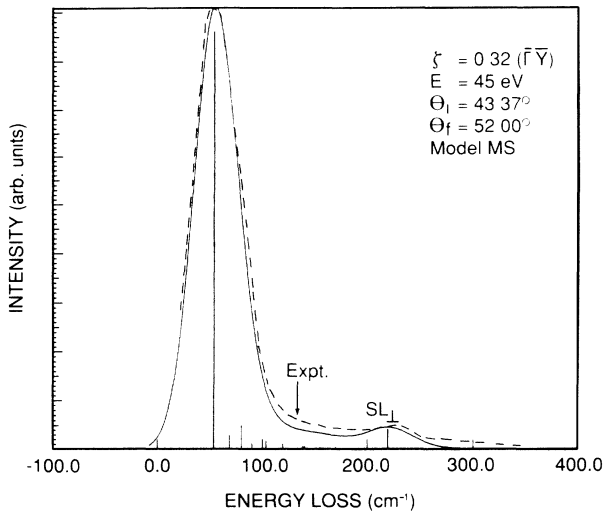

FIG. 6. Calculated (solid line) and measured (dashed line) electron-energy-loss cross-section spectra for $E=45$ eV and $\zeta=0.32$ along the $\bar{\Gamma}\,\bar{Y}$ direction. The surface-force-constant model (the MS model) is used to generate the phonon frequencies and eigenvectors. The surface-layer relaxation based on LEED analysis is included.

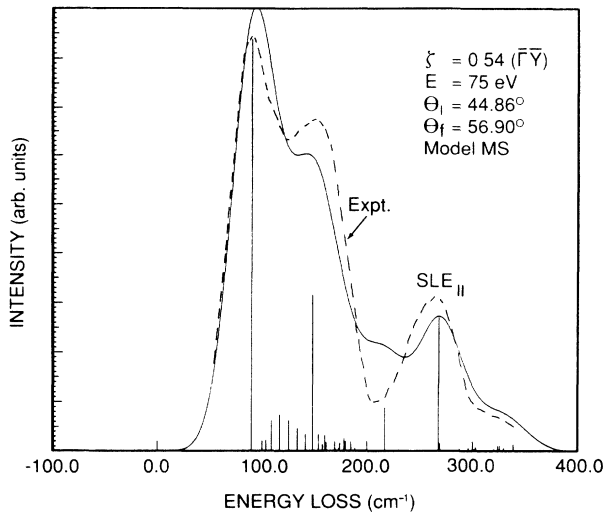

FIG. 8. Same as Fig. 6, but for $E=75$ eV and $\zeta=0.54$ along line $\bar{\Gamma}\,\bar{Y}$.

branches near $\bar{Y}$. The force constants of this surface-adjusted model (MS model) are listed in Table I of the preceding paper.[1] The full phonon dispersion curves using the MS model and its comparison with data are shown in Figs. 9 and 10 of the preceding paper. Here, to aid the identification of these modes in the discussion of electron-energy-loss cross sections in the next section, we show again in Figs. 1 and 2 the calculated and measured phonon dispersion curves along $\bar{\Gamma}\,\bar{Y}$ and $\bar{\Gamma}\,\bar{X}$, respectively. The calculation used the lattice-dynamical model MS.

III. ELECTRON-ENERGY-LOSS CROSS SECTIONS

In an electron-energy-loss cross-section calculation, the layer-by-layer atomic-displacement amplitudes of each phonon mode are used as inputs.[2–5] The cross sections are calculated at different phonon wave vectors, incident-electron energies, and scattering geometries. By comparing calculated cross sections with data over a wide range of the above conditions, we obtain stringent tests for the accuracy of the polarization and amplitude of the atomic displacements generated by a lattice-dynamical model.

We show in Figs. 3–5 the calculated electron-energy-loss cross-section spectra along the $\bar{\Gamma}\,\bar{Y}$ direction, for ζ $[=q_{\parallel}/(1.09\ \text{Å}^{-1})]=0.64$, 0.9, and 1.0, respectively. The incident-electron energy E and the angles of incidence and exit θ_i and θ_f are specified in each figure. The scattering plane is along the [110] direction. For these figures the bulk-force-constant model with surface-force balance (i.e., the MB model) is used. The large discrepancies are clearly evident. The lowest energy-loss peak in the theory falls significantly below that of the data. This

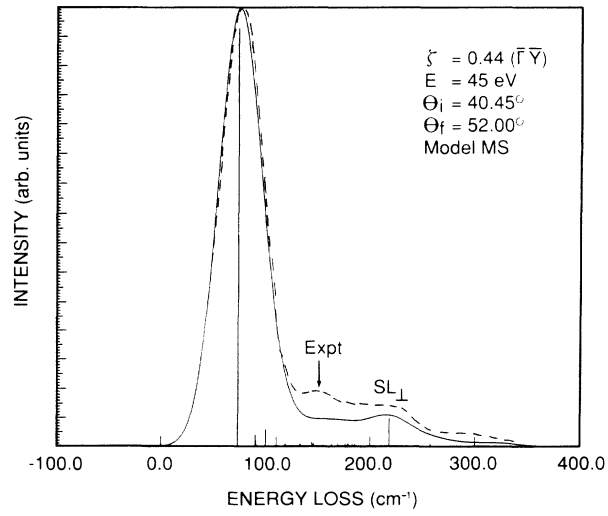

FIG. 7. Same as Fig. 6, but for $\zeta=0.44$ along line $\bar{\Gamma}\,\bar{Y}$.

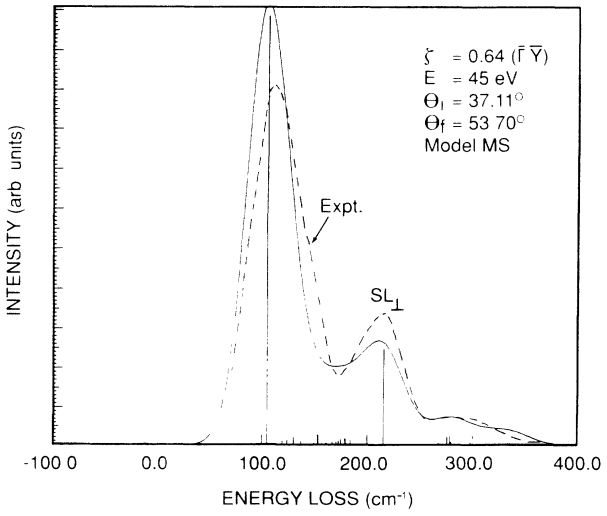

FIG. 9. Same as Fig. 6, but for $\zeta=0.64$ along line $\bar{\Gamma}\,\bar{Y}$.

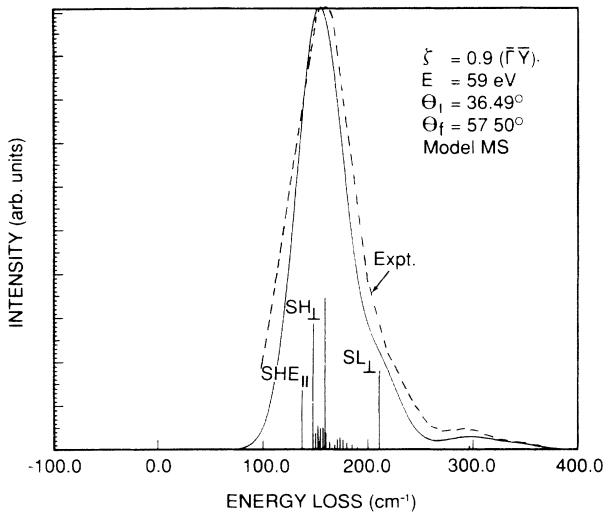

FIG. 10. Same as Fig. 6, but for $E=59$ eV and $\zeta=0.9$ along line $\bar{\Gamma}\,\bar{Y}$.

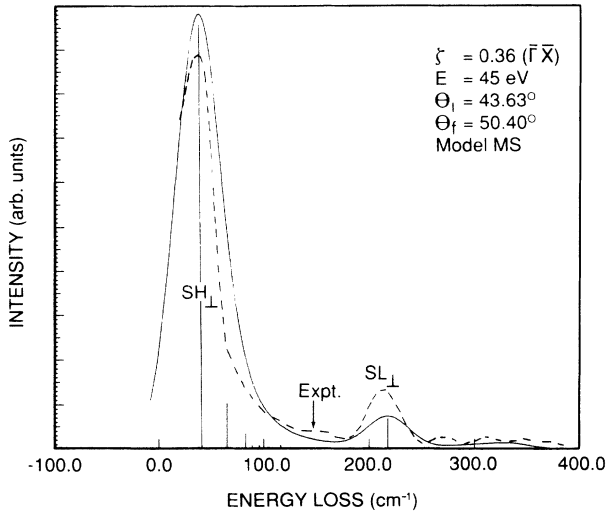

FIG. 12. Same as Fig. 6, but for $\zeta=0.36$ along the $\bar{\Gamma}\,\bar{X}$ direction.

peak in the theory is dominated by the Rayleigh mode ($SH_\perp$). In the lattice-dynamical model MB, the polarization of the Rayleigh mode at $\bar{Y}$ is predominantly perpendicular to the surface for the first-layer Ni atoms. At midzone, its polarization is mixed between parallel and perpendicular displacements. Figures 3–5 clearly show that such a model cannot explain the data. The loss energy of this peak must be shifted upward.

Figures 6–11 show the calculated EELS spectra using phonon frequencies and eigendisplacements from the optimal surface lattice-dynamical model MS. The calculated EELS spectra are compared to the data for different scattering conditions at $\zeta=0.32$, 0.44, 0.54, 0.64, 0.9, and 1.0, respectively. We note marked improvements in the agreement of the peak positions. It would be interesting to examine the polarization of the lowest-frequency surface mode in the MS model (see Table I of Ref. 1). Within the zone, e.g., $\zeta=0.32$–0.64, this lowest-frequency mode has the largest EELS cross section, and its first-layer Ni displacement has a strong perpendicular component. This is the Rayleigh mode. At $\zeta=0.9$ and 1.0 the lowest-frequency surface mode has a first-layer Ni displacement *parallel* to the surface (i.e., it has changed into a longitudinal mode). Near $\bar{Y}$, the next-higher-frequency mode, which is very close to the bulk band, has first-layer Ni displacement perpendicular to the surface. This higher-frequency mode has $SH_\perp$ character and shows a strong inelastic-electron-scattering strength in Figs. 10 and 11. The peak in the calculated EELS spectra (made up of individual inelastic-scattering cross sections, i.e., the vertical lines, broadened with a Gaussian function of full width at half maximum of 40 cm^{-1}) is now up-shifted in energy to agree with the data. We note from Fig. 11 that the peak in the EELS spectra does not

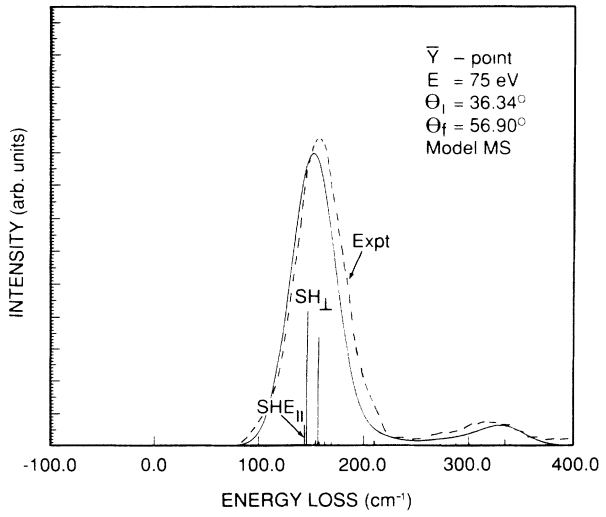

FIG. 11. Same as Fig. 6, but for $E=75$ eV and at the $\bar{Y}$ point.

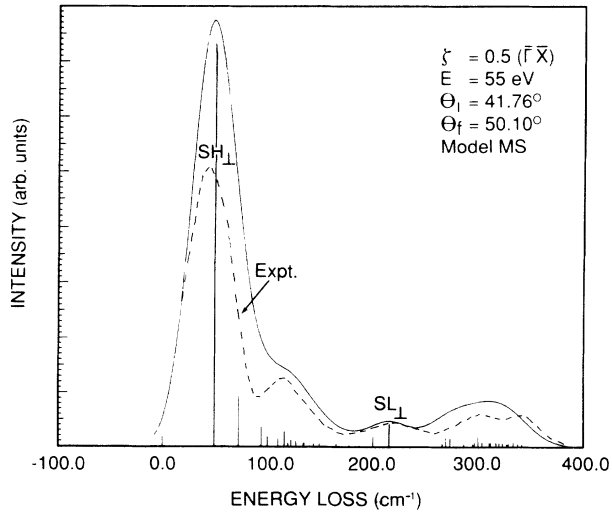

FIG. 13. Same as Fig. 6, but for $E=55$ eV and $\zeta=0.5$ along line $\bar{\Gamma}\,\bar{X}$.

line up with a particular phonon mode; instead, it is the result of a number of closely spaced surface, bulk, and resonance modes.

For completeness, we show in Figs. 12 and 13 the comparison between calculated EELS cross-section spectra using the lattice-dynamical model MS and the data for wave vectors along the $\bar{\Gamma}\bar{X}$ direction. Again, there is good agreement in the peak positions and general features between the calculated and measured spectra. In Figs. 1, 2, and 6–13 we show that the lattice-dynamical model MS produced dispersion curves in good agreement with the data. It also produced eigendisplacements whose calculated EELS cross sections are in good agreement with the measured spectra taken under different scattering conditions.

IV. SENSITIVITY OF EELS SPECTRA TO SURFACE GEOMETRY

As the data in the preceding paper[1] show, the EELS cross sections are sensitive functions of scattering conditions. This is because for a given phonon at wave vector $\mathbf{q}_{\parallel}$, while the layer-by-layer eigendisplacements are fixed, the coherent contributions of the loss amplitudes from each layer are sensitive functions of the electron wavelength and incident and exit angles, *as well as* the surface spacings. In the calculations of the preceding section the relaxed, rumpled surface geometry[8] was used. We show in this section that if we use the wrong surface geometry, we shall no longer obtain good agreement between theory and experiment in the EELS cross sections, *even* when we use the correct surface lattice-dynamical model.

In Figs. 14 and 15 we show the calculated EELS cross sections wherein the surface relaxation is neglected (i.e., an ideal bulk-terminated surface structure is used). All other parameters are kept the same as those used to generate the calculated results of Figs. 6–13. Upon comparison with experiment, we see a distinct, qualitative deterioration in the agreement. These figures demonstrate the importance of using the correct surface geometry in the comparison of EELS cross sections between theory and experiments. Conversely, it is clear that EELS cross sections can be used to determine the correct surface geometry. Such usage has been demonstrated for the Ni(001)-$c(2\times2)$S system.[5]

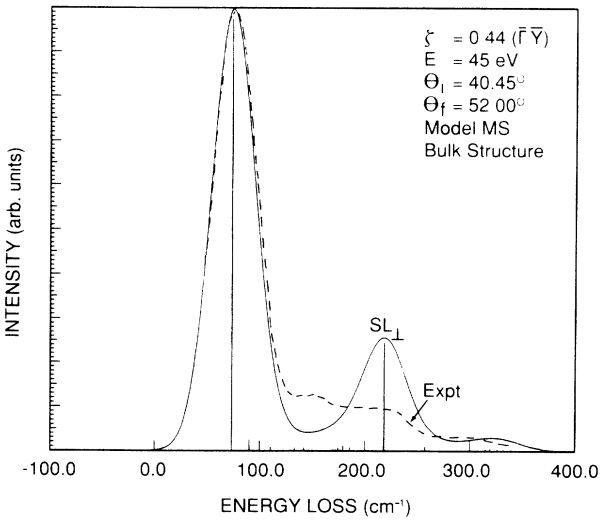

FIG. 14. Same as Fig. 7, but the surface structure is assumed to be bulklike.

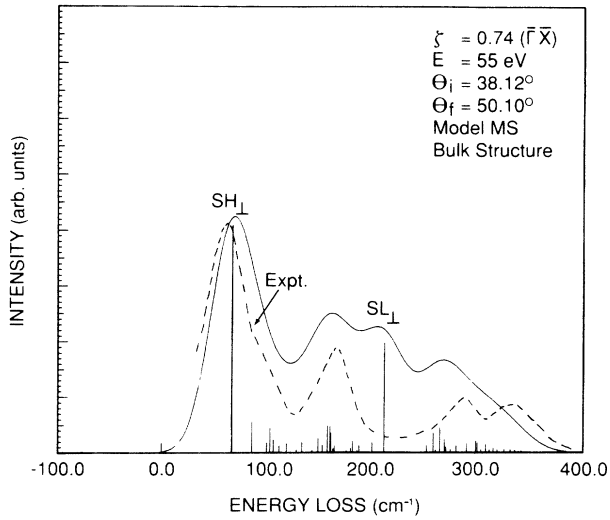

FIG. 15. Same as Fig. 14, but for $E=55$ eV and $\zeta=0.74$ along line $\bar{\Gamma}\bar{X}$.

On the NiAl(110) surface the lateral distance between coplanar Ni and Al atoms is shorter along the [100] direction. We found that calculated EELS cross sections with a scattering plane perpendicular to this closer-packed azimuth are more sensitive to the surface rumpling (i.e., Ni inward displacement and Al outward displacement) than the [110] azimuth. This phenomenon is related to the larger forward-scattering versus other-angle-scattering process. Such directional sensitivity has also been found in reflection high-energy electron diffraction (RHEED), for example.[10,11]

V. SUMMARY

We have shown that on the NiAl(110) surface significant surface force-constant adjustments are needed in the lattice-dynamical model. We presented results of a surface-adjusted force-constant model which produced phonon dispersion curves and EELS cross sections in good agreement with experiment. The surface-adjusted force-constant model produced a Rayleigh mode whose first-layer Ni polarization switched to pure longitudinal at point $\bar{Y}$. This behavior is supported by the data, and such a switch is not present in the Rayleigh mode calculated from bulk force constants.

The comparison between theory and experiment of the EELS cross sections allows detailed analysis of the polarizations of individual surface, bulk, and resonance modes. The contribution of a given mode to the measured spectra can be clearly identified. It also allows precise mapping of the dispersion curves, even for modes that are closely spaced in frequency. In principle, if there is a

sufficiently large database, it is possible to uniquely determine an optimal lattice-dynamical model that fits both the phonon dispersion curves and the inelastic-electron-scattering cross sections. In practice, one always works with a finite database. Then, the validity of the physical quantities obtained depends on the size of the database. For the present case of NiAl(110), the dispersion and EELS cross-section data are quite extensive. We believe that the physical quantities obtained, such as the layer-dependent mean-square atomic-displacement amplitudes and the phonon frequencies, should be rather reliable. We have also shown that the EELS cross-section analyses confirm the relaxed surface geometry found by LEED (Ref. 8) and MEIS.[9]

ACKNOWLEDGMENTS

This work was supported by the U.S. Department of Energy under Grant DE-FG02-84ER45147, and by Petroleum Research Fund Grant No. 1154-AC5,6, administered by the American Chemical Society.

---

*Present address: Department of Chemistry, University of Toronto, Lash Miller Chemical Laboratories, Toronto, Canada M5S 1A1.

[1]M. Wittig, W. Hoffmann, E. Preuss, R. Franchy, H. Ibach, Y. Chen, M. L. Xu, and S. Y. Tong, this issue, the preceding paper, Phys. Rev. B **42**, 5443 (1990).

[2]S. Y. Tong, C. H. Li, and D. L. Mills, Phys. Rev. Lett. **44**, 407 (1980); C. H. Li, S. Y. Tong, and D. L. Mills, Phys. Rev. B **21**, 3057 (1980).

[3]S. Y. Tong, C. H. Li, and D. L. Mills, Phys. Rev. B **24**, 806 (1981).

[4]M. L. Xu, B. M. Hall, S. Y. Tong, M. Rocca, H. Ibach, S. Lehwald, and J. E. Black, Phys. Rev. Lett. **54**, 1171 (1985).

[5]Z. Q. Wu, Y. Chen, M. L. Xu, S. Y. Tong, S. Lehwald, M. Rocca, and H. Ibach, Phys. Rev. B **39**, 3116 (1989).

[6]H. Ibach and D. L. Mills, *Electron Energy Loss Spectroscopy and Surface Vibrations* (Academic, New York, 1982).

[7]M. Mostoller, R. M. Nicklow, D. M. Zehner, S.-C. Lui, J. M. Mundenar, and E. W. Plummer, Phys. Rev. B **40**, 2856 (1989).

[8]J. R. Noonan and H. L. Davis, Phys. Rev. Lett. **59**, 1714 (1987).

[9]S. M. Yalisove and W. R. Graham, Surf. Sci. **183**, 556 (1987).

[10]S. Y. Tong, T. C. Zhao, H. C. Poon, K. D. Jamison, D. N. Zhou, and P. I. Cohen, Phys. Lett. **A128**, 447 (1988).

[11]K. D. Jamison, D. N. Zhou, P. I. Cohen, T. C. Zhao, and S. Y. Tong, J. Vac. Sci. Technol. A **6**, 611 (1988).